

Adjustable testing setup for a single-loop optoelectronic oscillator with an electrical bandpass filter

Mehmet Alp ILGAZ^{1,*}, Andrej LAVRIC¹, Temitope ODEDEYI²,
Izzat DARWAZEH², Bostjan BATAGELJ¹

¹Radiation and Optics Laboratory, Faculty of Electrical Engineering, University of Ljubljana, Ljubljana, Slovenia

²Department of Electronic and Electrical Engineering, University College of London, London, United Kingdom

Received: 26.07.2019

Accepted/Published Online: 27.11.2019

Final Version: 08.05.2020

Abstract: In this paper we present a novel method to measure the free spectral range (FSR) and side-mode suppression ratio (SMSR) of an optoelectronic oscillator (OEO) by adjusting the optical fiber length using an optical path selector and signal source analyzer. We have designed a setup for a single-loop OEO operating around 5 GHz and 10 GHz that features electrical bandpass filters for side-mode suppression. The proposed approach makes it possible to evaluate the FSR and SMSR of OEOs with different optical fiber paths without requiring the changing of fiber spools or optical connectors. This approach could be useful for testbeds that investigate the implementation of an OEO in a 5G radio access network.

Key words: Optical path selector, optoelectronic oscillator, phase noise, free spectral range, side-mode suppression ratio, electrical bandpass filter

1. Introduction

The optoelectronic oscillator (OEO) [1, 2] is a high-frequency oscillator capable of generating signals in the microwave (300 MHz to 30 GHz) and millimeter wave (30 GHz to 300 GHz) ranges. The device consists of optical and electrical components, as illustrated in Figure 1.

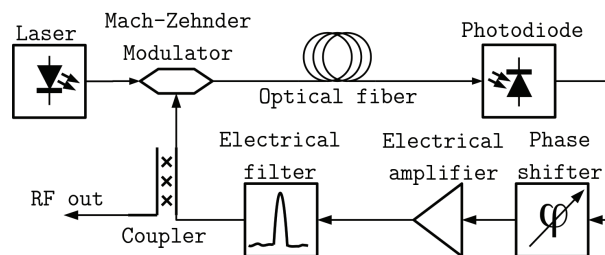


Figure 1. A basic configuration of the single loop OEO.

One of the main advantages of the OEO is that it generates a high-frequency signal with low phase noise due to having a high quality factor (Q-factor) based on a long optical delay line. The OEO commonly features an optical fiber as a delay line; however, there are some configurations featuring alternatives such as

*Correspondence: mehmet.ilgaz@fe.uni-lj.si

a whispering-gallery-mode resonator [3] or a spiral shape optical waveguide [4]. Another benefit of the OEO is that due to the properties of the resonator the level of the phase noise does not change with the frequency of the oscillation signal. The working principle of the OEO can be explained thus: the optical delay line works as a resonator and the electrical loop is used as a feedback, and if the Barkhausen conditions are satisfied, the OEO begins to oscillate at frequencies determined by the filter's properties. In other words, the filter determines the oscillation frequency when the other conditions (enough gain and correct phase) are met.

The main drawback of the OEO is the multimode operation of the oscillator. Besides the central oscillator signal, there are also side modes in the spectrum resulting from cavity multifrequency operation. The cavity modes appear in the output signal due to the nonideal behavior of the electrical bandpass filter of the single-loop OEO. The side-mode suppression ratio (SMSR) is defined as the power ratio between the oscillator signal and the closest side mode. The frequency difference between the main mode and the first side mode, defined as the free spectral range (FSR), is based on the optical fiber length used in the OEO's loop. When the fiber length is increased, the FSR becomes smaller, meaning that the side modes are closer to the main frequency, making it difficult to filter out the side modes. For the suppression of the side modes, some techniques to increase the Q-factor of the OEO's filtering have been developed; these include the dual-loop [5] or multiloop OEO [6] configuration. Besides using one or more additional optical loops, solutions such as injection locking [7], coupled-OEO [8], hybrid filtering [9], or using optical filters [10, 11] have been developed for the purpose of increasing the Q-factor of filtering of the OEO. There are also some electrical solutions such as the application of a quality multiplier [12, 13] to make the bandwidth of the electrical bandpass filter narrower. In general, these solutions have all been successfully implemented, but they require extra devices or references that increase the complexity of the single-loop OEO. Moreover, the adoption of photonic filters [14–16] increases the complexity of the optical part of the OEO.

In this paper we propose a new experimental setup to measure the FSR and SMSR quickly over a different optical fiber length, using microstrip-based electrical bandpass filters. With this, we will have a useful solution to design the OEO to use an optimum fiber length with an electrical filter. For design simplicity and cost effectiveness, we have adopted the microstrip electrical bandpass filter in our experimental study. There are some traditional analytical approaches for predicting the SMSR and FSR of the OEO signal [17, 18]. These analytical approaches require parameters such as the laser relative intensity noise and the impedance of the photodetector to determine the SMSR. These methods for a theoretical prediction require accurate knowledge of the parameter values of the used components, which are not easy to measure. The simplicity and directness of the approach proposed here advantageously provide an efficient method to measure the SMSR and FSR. To the best of our knowledge, this is the first time the combination of a single-loop OEO with an optical path selector has been proposed and applied for measuring the FSR and the SMSR for different optical fiber lengths. This paper is an extended version of the work presented in TELFOR 2018 [19] with additional measurement verification.

2. Experimental setup

The OEO uses long fiber lengths to achieve a high Q-factor, which is necessary to decrease the phase noise. However, there is a trade-off between the side modes and the phase noise of the OEO. In order to have a low phase noise OEO, the optical delay line should be longer. On the other hand, when the fiber length is increased

the modes become closer. The FSR is defined as

$$FSR = \frac{c_0}{n_g L}, \quad (1)$$

where c_0 is the speed of light in a vacuum, n_g is the refractive index of the optical fiber, and L is the optical fiber length. From this expression we see that the length of the optical fiber affects the FSR of the OEO signal. The longer the fiber, the closer the modes, necessitating the introduction of a filter with a very narrowband performance. This relation is shown in Figure 2.

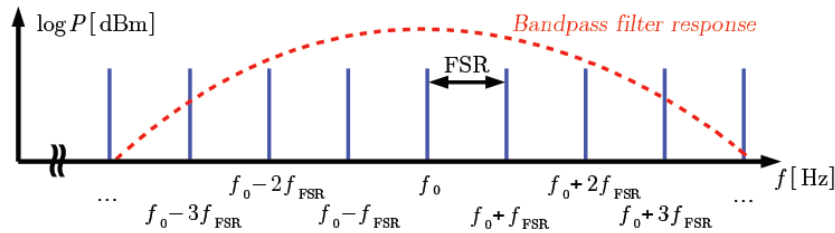


Figure 2. Filtering results based on the optical fiber length [19].

The output field of a Mach-Zehnder modulator (MZM) $E_{out}(t)$ [20] is given by

$$E_{out}(t) = E_0 \left\{ \cos\left(\frac{\beta\pi}{2}\right) \cos\left(\frac{\alpha\pi}{2} \cos \omega_{RF} t\right) - \sin\left(\frac{\beta\pi}{2}\right) \sin\left(\frac{\alpha\pi}{2} \cos \omega_{RF} t\right) \right\} \cos \omega_0 t, \quad (2)$$

where ω_{RF} is the modulation angular frequency, α is the normalized amplitude driving the MZM, β is the normalized bias, and ω_0 is the angular frequency of the optical carrier. In [18], the signal behavior of the OEO in the loop and its derivation are given in more detail.

We propose a setup to measure the FSR and SMSR of the OEO signal with different optical fiber lengths. The main advantage of this setup is that it provides a solution for designers with different results on the FSR, SMSR, and the phase noise of the OEO signal to select the optimum one in the design. The setup consists of a continuous-wave (CW) laser, a MZM, an erbium-doped fiber amplifier (EDFA), an optical path selector, three optical fibers (1.25 km, 2.5 km, and 5 km), a p-i-n photodetector, a phase shifter up to 18 GHz, electrical isolators, electrical amplifiers working between 4 GHz to 14 GHz, an electrical filter, and a signal source analyzer (SSA) up to 26.5 GHz. The configuration is shown in Figure 3.

In this setup we have used electrical isolators to avoid reflections and to block self-oscillations in the electrical loop of the OEO. We put the spectrum analyzer in the system to tune the phase shifter to provide conditions for oscillation, while the length of the optical fiber is changed by the optical path selector. Electrical amplifiers and the EDFA are used to compensate for the optical and electrical losses. With this setup we can easily measure the FSR and SMSR of the different electrical bandpass filters for different optical fiber lengths without changing the optical connectors. We prefer to use an SSA for measurements of the FSR and SMSR instead of a spectrum analyzer, because it provides results with an averaging possibility and a full spectrum. In addition, measuring with the SSA makes it possible to see the phase-noise spectrum of the OEO with a different

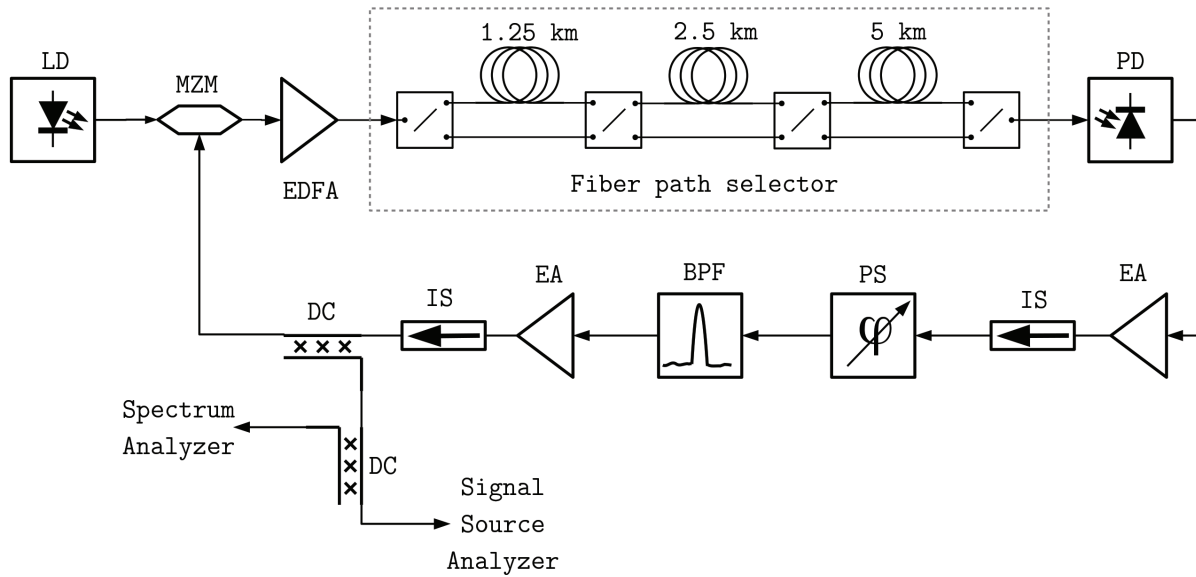


Figure 3. Diagram of the experimental setup to measure the FSR and SMSR. The insertion loss (IL) of the fiber path selector is around 3 dB (LD: laser diode, MZM: Mach-Zehnder modulator, EDFA: erbium-doped fiber amplifier, PD: photodiode, EA: electrical amplifier, IS: isolator, PS: phase shifter, BPF: bandpass filter, DC: directional coupler).

fiber length. The relation that describes the spectral density of the OEO [21] is

$$S_{RF}(\Delta f) = \frac{\delta}{(\delta/2\tau)^2 + (2\pi)^2(\tau\Delta f)^2}, \quad (3)$$

where τ is the total group delay of the OEO loop, Δf is the frequency offset from the oscillation frequency of the OEO, and δ is the input noise-to-signal ratio. In δ all the noise contributions are taken into consideration, i.e. the thermal noise, the shot noise, and the laser relative intensity noise. An exact equation for δ is given in Yao and Maleki [21].

The phase noise obtained with the described measuring setup is shown in Figure 4, with the phase-noise spectrum directly obtained from the SSA. With this measurement we can easily obtain a phase noise of -94.2 dBc/Hz at a 1-kHz frequency offset from the carrier and -123.9 dBc/Hz at 10 kHz. These offsets are widely used for a comparison of the phase noise in the literature. In addition, we can also measure the FSR and SMSR of the OEO's signal.

3. The importance of side modes for a 5G radio access network

A possible approach for the implementation of a single-loop OEO in a 5G radio access network (RAN) is defined in a previous study [22]. In this implementation one of the crucial parameters is the bandwidth of the electrical bandpass filter, since it affects the SMSR of the OEO's signal. Therefore, we experimentally study the electrical bandpass filter in the single-loop OEO with a measurement of the SMSR and FSR. In our implementation we have kept the design of the filters as simple as possible to minimize the cost and complexity of the 5G RAN. As the challenges with side modes are one of the more critical demands of the 5G RAN, since they affect the spectral efficiency, we think that our approach for the measuring system would be useful in selecting the

appropriate electrical bandpass filter for the single-loop OEO that will be implemented in the 5G RAN. The concept is shown in Figure 5.

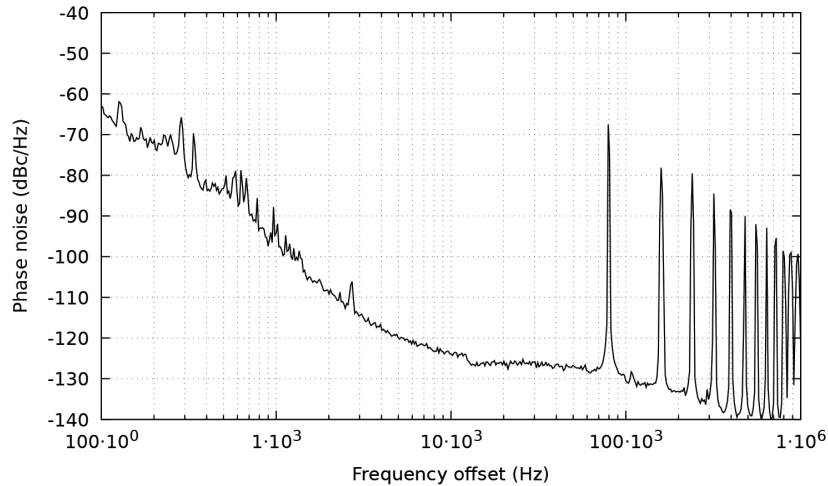


Figure 4. Phase-noise spectrum of the OEO with a fiber length of 2.5 km.

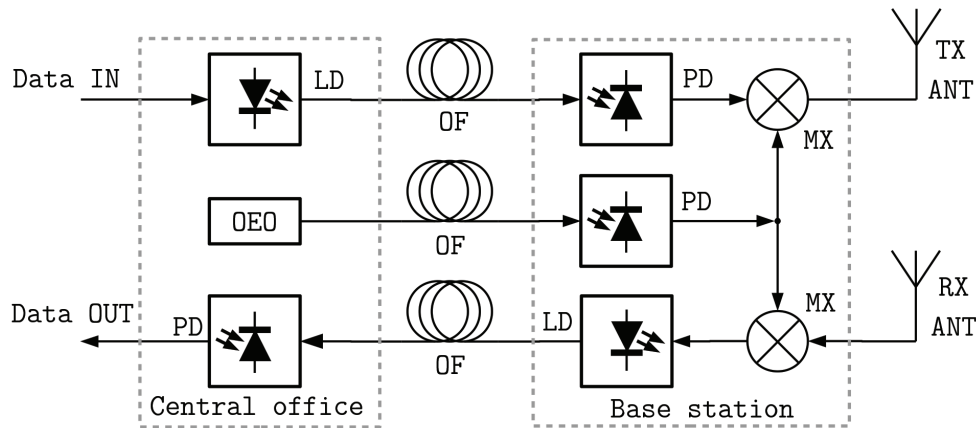


Figure 5. Possible idea for the implementation of a 5G RAN with an OEO in the central office and distributed to a base station (LD: laser diode, OF: optical fiber, PD: photodiode, MX: mixer, TX ANT: transmitter antenna, RX ANT: receiver antenna, OEO: optoelectronic oscillator).

Figure 5 indicates that there is a possibility to implement the OEO in the central station of the 5G RAN and deliver its signal to base stations of the 5G RAN. In other words, the low-phase-noise OEO’s signal is distributed from the central station to the base station via fiber-optic links. The single OEO can provide that signal to multiple base stations via optical splitters.

4. Measurement results

In the experimental setup we built up the OEO at two different operating frequencies, around 5 GHz and 10 GHz, and measured the FSR and SMSR of the output signal. The experimental setup is shown in Figure 6.

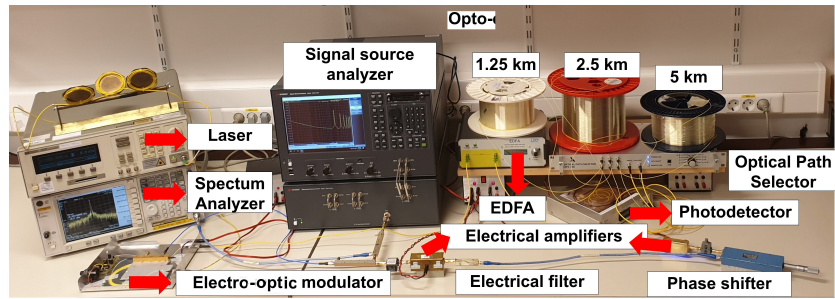


Figure 6. Photograph of the measurement setup to measure the FSR and SMSR by fiber path selector.

The electrical-bandpass-filter-based microstrip-line configuration generally has a Q-factor below 200, which is very low for the filtering of a single-loop OEO in the microwave and millimeter wave ranges, where the FSR of the OEO modes are between 200 kHz and 10 kHz for 1 km to 15 km of optical fiber, respectively. Apart from the frequency response of the filter, which can be analytically predicted, the Q-factor of the fabricated filter can also be affected by factors related to design and manufacturing. These factors include the manufacturing process adopted, i.e. chemical etching or laser production, the quality of the SMA connectors used, the resolution of the mask used in the manufacturing, etc. In our experimental setup we measured the FSR and SMSR of the electrical bandpass filters fabricated using different manufacturing processes. We used an RO4350 substrate¹ for our microstrip filters. Photographs of the electrical bandpass filters used in the experimental setup are shown in Figure 7.

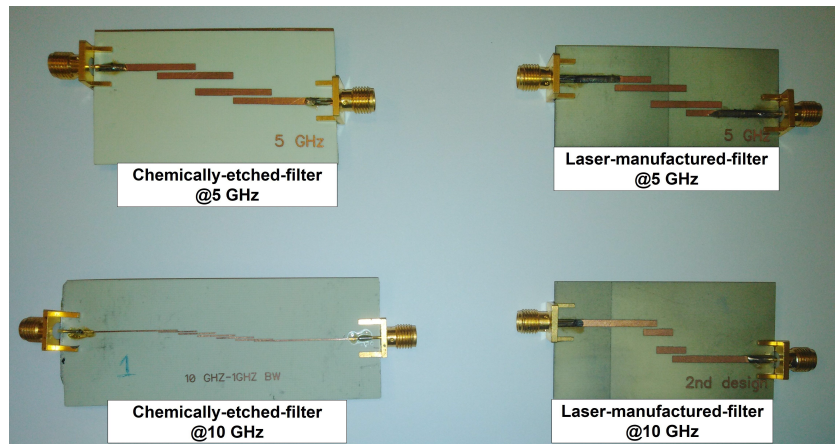


Figure 7. Photograph of the electrical bandpass filters for the measurements.

4.1. Single-loop OEO at 5 GHz

In the first experiment we set up measurements to measure the FSR and SMSR of the single-loop OEO with a chemically etched electrical bandpass filter and the OEO with a laser manufactured electrical bandpass filter. These electrical bandpass filters are designed with the well-known Chebyshev filter characteristics. For each

¹Rogers Corporation (2019). Datasheet of RO4000 Series High Frequency Circuit Materials [online]. Website <https://rogerscorp.com/-/media/project/rogerscorp/documents/advanced-connectivity-solutions/english/data-sheets/ro4000-laminates-ro4003c-and-ro4350b---data-sheet.pdf> [accessed 03 December 2019].

measurement we changed the optical fiber length from 1.25 km to 8.75 km with an increment of 1.25 km. Since the electrical bandpass filter and the fiber spool insert an additional phase shift into the OEO loop, the biasing of the MZM and phase shifter has to be tuned for each measurement to provide the oscillation conditions.

4.1.1. Laser-manufactured filter-based single-loop OEO at 5 GHz

For the first measurement we inserted into the OEO's loop a filter produced by a fast and accurate laser-based prototyping system. While the filter was analytically designed to operate at 5 GHz, due to the material tolerance and the difference between the simulation results and the measurement process, the fabricated device has a measured central frequency of 4.670 GHz and a 3-dB bandwidth of 160 MHz. Measurements of the FSR and SMSR using our proposed experimental setup are shown in Table 1. In this case the filter is manufactured with a LPKF ProtoLaser S4 that operates at a green laser 532-nm wavelength, with a pulse frequency varying from 25 kHz to 300 kHz and with a manufacturing accuracy of $\pm 1.98 \mu\text{m}$.²

4.1.2. Chemically etched filter-based single-loop OEO at 5 GHz

For the second measurement we put a chemically etched filter in the OEO's loop. As mentioned previously, the filter was analytically designed to operate at 5 GHz, but also in this case the manufactured device has a shifted measured central frequency of 4.675 GHz and a 3-dB bandwidth of 130 MHz due to the material tolerances and disagreement between the computation and the experimental measurement. Measurements of the FSR and SMSR are shown in Table 1. The filter is manufactured by traditional chemical etching using ferrite chloride (FeCl_3).

Table 1. Measurement results of the FSR and SMSR for a 5-GHz OEO.

	Theoretical calculation	Experimental result	Laser-manufactured	Chemically etched
Fiber length [km]	FSR [kHz]	FSR [kHz]	SMSR [dB]	SMSR [dB]
1.25	163.50	156.24	78.05	75.33
2.5	81.75	79.29	70.42	64.68
3.75	54.50	53.54	67.31	61.65
5	40.88	40.24	65.55	60.59
6.25	32.70	32.48	59.63	58.64
7.5	27.25	27.17	57.05	57.56
8.75	23.36	23.14	51.98	57.21

4.1.3. Evaluation

From the measurement result it is clear that the FSR follows the theoretical calculation obtained with Eq (1). For the SMSR, the laser-manufactured filter has a better response when the optical fiber length is up to 6.25 km and the chemically etched filter has a better response when the optical fiber lengths are 7.5 km and 8.75 km. According to this result, the designer can select the appropriate filtering for the OEO. The main focus of the present paper is on the new approach of the OEO to the FSR and SMSR measurement; however, it is worthwhile commenting on the differences in the measured properties of the chemically and laser-manufactured filter in their 3-dB points and central frequency. These are attributed to the fact that although laser manufacturing has the advantage of tens-of-microns tolerances, chemical etching is generally limited to

²LPKF Laser & Electronics (2019). Brochure of LPKF ProtoLaser S4 [online]. Website https://www.lpkfusa.com/datasheets/prototyping/FLY_ProtoLaser_S4_EN.PDF [accessed 03 December 2019].

hundreds of microns, and the laser process causes thermal stress on the PCB, which could change the metal properties. On the other hand, chemical etching does not significantly alter the metal properties of the PCB and hence, given the dimensions of the manufactured filters, the less accurate chemical process results are closer to the design/simulations predictions than the laser process.

4.2. Single-loop OEO at 10 GHz

For measurement at 10 GHz, we again use two different manufacturing processes, but in this case with two different filter designs. For the purpose of presenting the operation of the single-loop OEO oscillating at 10 GHz, we used microstrip filters with different designs. Even in this case of measurements we have optical fiber length from 1.25 km to 8.75 km with an increment of 1.25 km. We changed one of the electrical amplifiers from the 5-GHz setup to provide an oscillation for 10-GHz filters, since they have different insertion losses compared to the 5-GHz ones. For each measurement we tuned the bias of the MZM and tuned the phase shifter to provide oscillations.

4.2.1. Laser-manufactured filter-based single-loop OEO at 10 GHz

In the third measurement we put a laser-manufactured filter on the loop of our OEO setup. While the filter was analytically designed to operate at 10 GHz, due to the material tolerance and the difference between the simulation results and the measurement process the device has a measured central frequency of 10.68 GHz and a 3-dB bandwidth of 461 MHz. The filter was manufactured using the same laser printing setup as used for the 5-GHz filter described in 4.1.1. Measurements of the FSR and SMSR are shown in Table 2.

Table 2. Measurement results of the FSR and SMSR for a 10-GHz OEO.

	Theoretical calculation	Experimental result	Laser-manufactured	Chemically etched
Fiber length [km]	FSR [kHz]	FSR [kHz]	SMSR [dB]	SMSR [dB]
1.25	163.50	158.49	73.39	78.10
2.5	81.75	79.29	68.79	71.08
3.75	54.50	53.54	58.52	67.22
5	40.88	40.24	53.72	62.50
6.25	32.70	32.48	52.48	48.94
7.5	27.25	27.17	48.79	39.88
8.75	23.36	23.14	47.10	38.21

4.2.2. Chemically etched filter-based single-loop OEO at 10 GHz

For the fourth measurement we put a chemically etched filter on the OEO's loop. The manufactured filter has a measured central frequency of 9.63 GHz and a 3-dB bandwidth of 585 MHz, which differs from the designed 10 GHz due to already mentioned tolerances. The filter was manufactured using the same etching process adopted for the 5-GHz filter described in 4.1.2. Measurements of the FSR and SMSR are shown in Table 2, where they can be compared with results achieved with measurements using the laser-manufactured filter.

4.2.3. Evaluation

As a result of the measurement in this experimental setup, the FSR is the same for different filters, since the optical fiber length is the same and the bandwidth of the electrical bandpass filter does not impact on the

results. However, due to the different designs of the filters, the SMSR should not be compared, since the filters were designed in different configurations. Nevertheless, from the results obtained in our experiments, we do not advise the use of OEOs with an optical length of more than 6.25 km for a laser-manufactured filter and 5 km for a chemically etched filter since it is generally accepted that SMSR should be greater than 50 dB.

5. Conclusion

Motivated by the complexity of current measurement techniques for the FSR and SMSR of the OEO, we developed a very fast, adjustable method to measure both parameters in a configuration with different optical fiber lengths. The newly proposed method provides time savings for the experimental setups with different electrical filters. In addition, this novel technique makes it possible to measure the phase noise of the OEO, which has an inverse relation to the optical delay line length. On the other hand, the longer fiber lengths result in the side modes becoming closer to the main mode. We think that the proposed setup will be helpful in the selection of electrical bandpass filters to overcome this trade-off. We also made measurements to see the effects on the different manufacturing processes for the electrical bandpass filters.

In our future work we would like to implement this idea for a more complicated configuration of the OEO, such as a multiloop OEO or injection-locked OEO to determine the appropriate lengths of the optical fiber in the loop to suppress the SMSR efficiently.

Acknowledgments

The authors would like to express their gratitude to the company InLambda BDT d.o.o. for the research equipment and devices. In addition, the authors would like to express their gratitude to the University College London for manufacturing the microstrip line electrical bandpass filters. Moreover, we would like to thank LPKF d.o.o for the laser manufacturing of the electrical bandpass filters. The work presented in this article is part of the FiWiN5G Innovative Training Network, which has received funding from the European Union's Horizon 2020 Research and Innovation Programme 2014–2018 under the Marie Skłodowska-Curie Action grant agreement No. 642355. The authors also acknowledge the financial support from the Slovenian Research Agency (research core funding No. P2-0246).

References

- [1] Yao XS, Maleki L. High frequency optical subcarrier generator. *Electronics Letters* 1994; 30 (18): 1525-1526. doi: 10.1049/el:19941033
- [2] Yao XS, Maleki L. Optoelectronic oscillator for photonic systems. *IEEE Journal of Quantum Electronics* 1996; 32 (7): 1141–1149. doi: 10.1109/3.517013
- [3] Maleki L. The opto-electronic oscillator (OEO): review and recent progress. In: 2012 European Frequency and Time Forum; Gothenburg, Sweden; 2012. pp. 497-500. doi: 10.1109/EFTF.2012.6502432
- [4] Tang J, Hao T, Li W, Domenech D, Banos R et al. Integrated optoelectronic oscillator. *Optics Express* 2018; 26 (9): 12257-12265. doi: 10.1364/OE.26.012257
- [5] Shao Y, Han X, Bing Y, Li M, Gu Y et al. Polarization multiplexed dual-loop OEO based on a phase-shifted fiber bragg grating. In: 2017 International Topical Meeting on Microwave Photonics (MWP); Beijing, China; 2017. pp. 1-4. doi: 10.1109/MWP.2017.8168340
- [6] Banky T, Horvath B, Berceli T. Optimum configuration of multiloop optoelectronic oscillators. *Journal of the Optical Society of America B* 2006; 23 (7): 1371-1380. doi: 10.1364/JOSAB.23.001371

- [7] Okusaga O, Adles EJ, Levy EC, Zhou W, Carter GM et al. Spurious mode reduction in dual injection-locked optoelectronic oscillators. *Optics Express* 2011; 19 (7): 5839-5854. doi: 10.1364/OE.19.005839
- [8] Dahan D, Shumakher E, Eisenstein G. Self-starting ultralow-jitter pulse source based on coupled optoelectronic oscillators with an intracavity fiber parametric amplifier. *Optics Letters* 2005; 30 (13): 1623-1625. doi: 10.1364/OL.30.001623
- [9] Liu A, Liu J, Dai J, Dai Y, Yin F et al. Spurious suppression in millimeter-wave OEO with a high-Q optoelectronic filter. *IEEE Photonics Technology Letters* 2017; 29 (19): 1671-1674. doi: 10.1109/LPT.2017.2742662
- [10] Ozdur I, Mandridis D, Hoghooghi N, Delfyett PJ. Low noise optically tunable opto-electronic oscillator with Fabry-Perot etalon. *Journal of Lightwave Technology* 2010; 28 (21): 3100-3106. doi: 10.1109/JLT.2010.2076773
- [11] Merrer PH, Llopis O, Bonnefont S, Ghisa L, Dumeige Y et al. Microwave filtering using high Q optical resonators. In: 2008 38th European Microwave Conference; Amsterdam, the Netherlands; 2008. pp. 381-384. doi: 10.1109/EUMC.2008.4751468
- [12] Bogataj L, Vidmar M, Batagelj B. Opto-electronic oscillator with quality multiplier. *IEEE Transactions on Microwave Theory and Techniques* 2016; 64 (2): 663-668. doi: 10.1109/TMTT.2015.2511755
- [13] Ilgaz MA, Bogataj L, Batagelj B, Vidmar M. Electronic stabilization methods for a single-loop optoelectronic oscillator. In: 2016 11th European Microwave Integrated Circuits Conference (EuMIC); London, United Kingdom; 2016. pp. 464-467. doi: 10.1109/Eu MIC.2016.7777592
- [14] Strekalov D, Aveline D, Yu N, Thompson R, Matsko AB et al. Stabilizing an optoelectronic microwave oscillator with photonic filters. *Journal of Lightwave Technology* 2003; 21 (12): 3052-3061. doi: 10.1109/JLT.2003.821724
- [15] Jiang F, Wong JH, Lam HQ, Zhou J, Aditya S et al. An optically tunable wideband optoelectronic oscillator based on a bandpass microwave photonic filter. *Optics Express* 2013; 21 (14): 16381-16389. doi: 10.1364/OE.21.016381
- [16] Romeira B, Kong F, Li W, Figueiredo JML, Javaloyes J et al. Broadband chaotic signals and breather oscillations in an optoelectronic oscillator incorporating a microwave photonic filter. *Journal of Lightwave Technology* 2014; 32 (20): 3933-3942. doi: 10.1109/JLT.2014.2308261
- [17] Hosseini SE, Banai A. Analytical prediction of the main oscillation power and spurious levels in optoelectronic oscillators. *Journal of Lightwave Technology* 2014; 32 (5): 978-985. doi: 10.1109/JLT.2013.2295758
- [18] Yao XS, Maleki L. Optoelectronic microwave oscillator. *Journal of the Optical Society of America B* 1996; 13 (8): 1725-1735. doi: 10.1364/JOSAB.13.001725
- [19] Ilgaz MA, Batagelj B. Measurement of the free spectral range and the side-modes suppression ratio of a 9.3-GHz single-loop opto-electronic oscillator by fiber path selector. In: 2018 26th Telecommunications Forum (TELFOR); Belgrade, Serbia; 2018. pp. 1-4. doi: 10.1109/TELFOR.2018.8611856
- [20] Hilt A. Microwave harmonic generation in fiber-optical links. In: 13th International Conference on Microwaves, Radar and Wireless Communications. MIKON - 2000. Conference Proceedings (IEEE Cat. No.00EX428); Wroclaw, Poland; 2000. pp. 693-698. doi: 10.1109/MIKON.2000.914029
- [21] Yao S, Maleki L. New results with the opto-electronic oscillators (OEO). In: Proceedings of 1996 IEEE International Frequency Control Symposium; Honolulu, HI, USA; 1996. pp. 1219-1222. doi: 10.1109/FREQ.1996.560316
- [22] Ilgaz MA, Batagelj B. Preliminary idea for a converged fixed and mobile network infrastructure with 5G using radio-over-fiber technology and an opto-electronic oscillator in the millimeter-wave range. In: 2016 18th International Conference on Transparent Optical Networks (ICTON); Trento, Italy; 2016. pp. 1-4. doi: 10.1109/ICTON.2016.7550476